Paper title: Progress of Inverted Metamorphic III-V Solar Cell Development at Spectrolab
Preferred area: 6 Space PV Cells and Systems
Presentation preference: Oral
Authors: Hojun Yoon, Moran Haddad, Shoghig Mesropian, Jason Yen, Kenneth Edmondson, Daniel Law, Richard R. King, Dhananjay Bhusari, Andreea Boca, and Nasser H. Karam
Affiliation: Spectrolab, Inc., 12500 Gladstone Avenue, Sylmar, CA 91342, USA
Telephone and email: (818) 838-7490, email: hyoon@spectrolab.com

Progress of Inverted Metamorphic III-V Solar Cell Development at Spectrolab

Hojun Yoon, Moran Haddad, Shoghig Mesropian, Jason Yen, Kenneth Edmondson, Daniel Law, Richard R. King, Dhananjay Bhusari, Andreea Boca, and Nasser H. Karam

Spectrolab, Inc., 12500 Gladstone Avenue, Sylmar, CA 91342, USA

ABSTRACT

Inverted metamorphic (IMM) solar cells based on III-V materials have the potential to achieve solar conversion efficiencies that are significantly higher than today's state of the art solar cells which are based on the 3-junction GaInP/GaInAs/Ge design. The 3J IMM device architecture based on (Al)GaInP/GaInAs/GaInAs, for example, allows for a higher voltage solar cell by replacing the low bandgap Ge (0.67 eV) from the conventional 3J structure with the higher bandgap (~1 eV) metamorphic GaInAs. The inverted growth simply allows the lattice-matched junctions (i.e., (Al)GaInP/GaInAs) to be grown first on the growth substrate, thereby minimizing or shielding them from the defects that arise from the metamorphic layers. We have demonstrated 30.5% AM0 efficiency based on the 3J IMM cell architecture grown on a Ge substrate, with V_{oc} = 2.963V, J_{sc} = 16.9 mA/cm^2, and FF = 82.5%. In addition, 4J IMM cells have been demonstrated with V_{oc} of 4.0 V. With additional development, demonstrating 33% AM0 efficiency is expected in the near future. However, the IMM devices demand more complex processing requirements than conventional solar cells, and we demonstrate the capability to fabricate large area solar cells from standard Ge solar cell substrates.

Introduction

Multijunction solar cells based on III-V materials grown lattice matched to Ge substrates have been commercially available to the space industry for the past decade, with beginning-of-life AM0 production efficiency improving from ~22% for dual-junction cells in 1997, to nearly 30% for the latest triple junction cells ("XTJ" cells, see reference [1]). While these lattice-matched cell architectures have proven themselves with as much as 10 years of flight heritage, it is well known that one of the biggest factors that makes the 3J cell efficiency far from ideal, is the low bandgap (E_g = 0.67 eV) of the Ge which serves as the 3rd junction as well as the substrate. This limitation is effectively mitigated by using the inverted metamorphic approach (IMM), by replacing the Ge subcell with a higher bandgap (~1.0 eV) subcell.

While ~1.0 eV is the near ideal bandgap for the 3rd junction in a 3J cell (e.g., ~1.9/1.4/~1.0 eV), or for the 4th junction in a 4J cell (e.g., ~2.0/1.7/1.4/~1.0 eV), it is also well suited for 5-6 junction cell architectures [2]. In lattice-matched structures, dilute GaInNAs material offers the ~1.0 eV bandgap with reasonable material quality, but has proven difficult to achieve high performance devices based on these cell architectures. Using lattice-mismatched, or metamorphic materials, for example, $Ga_{1-x}In_xAs$, a ~1.0 eV bandgap can be readily achieved but has a rather large lattice mismatch (~2%) with the Ge (or GaAs) substrate, and hence it is inherently more difficult to grow this material with high quality. However, low or moderately mismatched materials can be grown to produce high efficiency solar cells, as recently demonstrated by the 40.7% efficient terrestrial solar cell [3] measured under concentration. A larger problem arises particularly for the highly mismatched layers, when this metamorphic material is incorporated into a conventional (upright) structure with lattice matched upper junctions: because the metamorphic $Ga_{1-x}In_xAs$ material is grown first, the material quality of the subsequent epitaxial layers can be compromised so that the overall device performance is impacted. Hence, by growing this device structure inverted, the lattice matched upper junctions are grown first on a pristine substrate surface, followed by the metamorphic $Ga_{1-x}In_xAs$ junction. In this way, the material and device quality of the lattice matched junctions can be preserved.

Table I provides a comparison of the performance parameters for Spectrolab's Ultra Triple Junction (UTJ) solar cell (highest performance product presently in production) and the 3J IMM cell (achieved to date and target). Various groups have recently reported [4,5,6] promising demonstrations using this IMM approach, suggesting that this technology may serve as the platform for the next-generation high efficiency solar cells.

Table I. Comparison of the performance parameters for Spectrolab's production UTJ cell (typical and best) and the 3J IMM cell (achieved and target).

	UTJ (typical)	3J IMM (achieved)	3J IMM (target)
V_{oc} (V)	2.66	2.963	3.05
J_{sc} (mA/cm^2)	17.1	16.9	17.2
Fill Factor (%)	84.0	82.5	85.0
AM0 Efficiency (%)	28.2	30.5	33.0

Although the IMM structure has a superior performance potential, it requires additional cell processing steps that present some challenges and fortuitously, some benefits. The inverted structure must first be mounted or bonded to a handle substrate, and the original growth substrate must be removed. From this point, virtually the same cell processing techniques used to fabricate conventional multijunction cells can be applied. While the extra steps make processing of the IMM devices more demanding, they naturally enable production of high areal (W/m^2) and specific power (W/kg) solar cells that are often desired for space applications, simply by employing light-weight handle substrates.

This paper presents Spectrolab's progress in the development of the IMM technology, based on MOVPE (metal organic vapor phase epitaxy) growth of III-V materials on standard Ge solar cell substrates (175 micron thick, 100 mm diameter). Specifically, the issue of the current density requirement of the ~1 eV junction is addressed. Advances in cell processing, in particular, handle mounting process, are presented that demonstrate the feasibility toward realizing 33% AM0 efficiency, large area IMM solar cells.

Characteristics of the IMM structure

Figure 1 highlights some of the key characteristics of a 3J IMM solar cell structure, compared to a conventional 3J cell structure. Schematics of as-grown layer structures are shown for (a) conventional 3J solar cell and (b) 3J IMM solar cell. A 4J IMM solar cell would comprise of an additional junction with a nominal bandgap of ~1.65-eV inserted between the top and middle subcells as shown in (b). The bandgap (eV) and the nominal strain (%) relative to the Ge substrate of the primary layers are also plotted (here, positive strain values represent compressive stress). In both cases, the "Top" and "Middle" subcells (labeled as "1" and "2") are based on lattice matched GaInP and GaInAs materials. For the conventional 3J, the "Bottom" subcell is Ge, which also serves as the substrate, while for the IMM, it is based on metamor-

phic $Ga_{1-x}In_xAs$. The selection of the exact composition is dependent primarily on whether a 3J or 4J IMM structure is desired. A compositionally graded buffer layer (labeled as "B") is employed to gradually transition the lattice constant from the middle cell to the metamorphic $Ga_{1-x}In_xAs$ bottom cell, in an attempt to minimize the dislocation density at the end of the buffer layer. The buffer layer material is selected such that it is sufficiently transparent (optically) for the metamorphic $Ga_{1-x}In_xAs$ bottom cell. As indicated in Figure 1(b), the strain is monotonically increased throughout the buffer, while the bandgap is held constant at a value significantly higher than that of the metamorphic bottom cell. While materials such as AlGaInAs and GaInP meet these requirements, the former has been used for the work reported here.

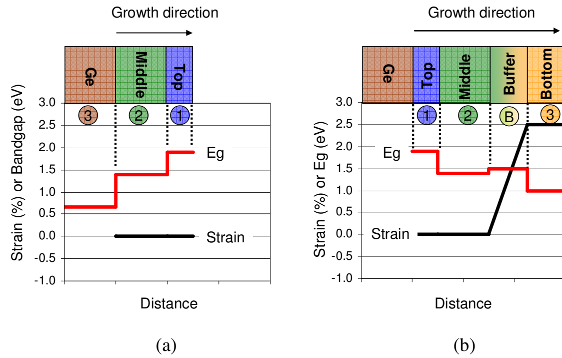

Figure 1. Schematic of as-grown (a) conventional 3J solar cell compared to (b) 3J IMM solar cell (a 4J IMM solar cell would comprise of an additional junction with a nominal bandgap of ~1.65-eV inserted between the top and middle subcells). The bandgap (eV) and the nominal strain (%) relative to the Ge substrate of the primary layers are also plotted. In these plots, positive strain values represent compressive stress.

The appropriate bandgap for the metamorphic $Ga_{1-x}In_xAs$ bottom cell is selected based on the empirically derived relationship between E_g and x as shown in Figure 2, and described by the equation:

$$E_g(x) = 0.413x^2 - 1.469x + 1.415$$

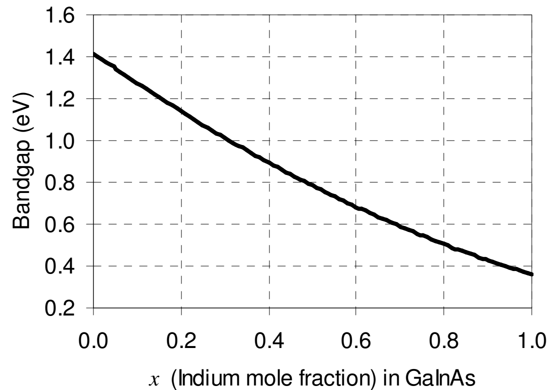

Figure 2. Empirically derived relationship between bandgap and Indium mole fraction in $Ga_{1-x}In_xAs$. Photoluminescence and HRXRD were used to independently measure the E_g and the lattice constants of $Ga_{1-x}In_xAs$ materials with various compositions.

The structural properties of these epitaxial layers in terms of composition, crystal quality, strain, and relaxation can be conveniently characterized using high resolution x-ray diffraction (HRXRD). Figure 3 provides an example of this characterization, in which (a) shows a (004) reflection triple axis ω-2θ scan and (b) shows a (115) glancing exit reciprocal space map (RSM). While both scans identify the substrate, buffer, and the metamorphic cell layers, the RSM uniquely reveals that the metamorphic buffer layers are fully relaxed.

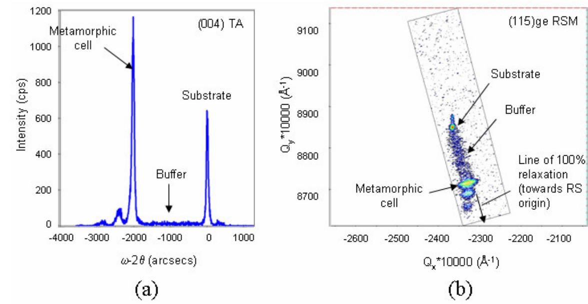

Figure 3. High resolution x-ray diffraction characterization of a typical 3J IMM device structure. (a) shows (004) triple axis ω-2θ scan and (b) shows (115) glancing exit reciprocal space map, revealing that the metamorphic layers are fully relaxed.

Current density requirement for the ~1 eV junction

Figure 4 shows the AM0 spectrum and the cumulative available current density curve starting from 890 nm. Wavelengths below 890 nm are assumed to be entirely absorbed by the upper subcells (e.g., GaInP/GaInAs). As noted in the plot, at 1.0 eV as an example, 19.9 mA/cm^2 is available from the AM0 spectrum.

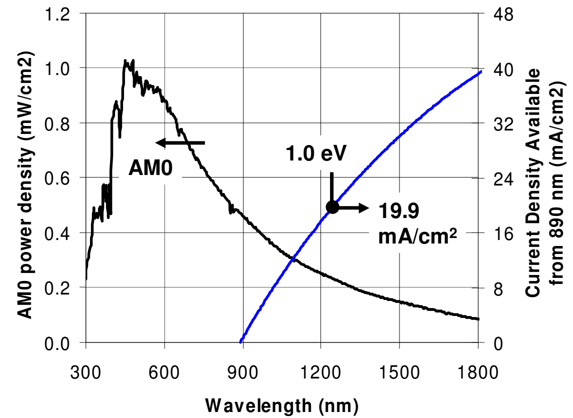

Figure 4. AM0 spectrum and cumulative available current density starting from 890 nm. Wavelengths below 890 nm are assumed to be entirely absorbed by the upper subcells (e.g., GaInP/GaInAs).

Observation of Figure 4 suggests that for a 3J IMM cell, a bandgap of 1.0 eV or lower is desired so that slight excess current can be produced by the bottom subcell. Because of the inherently lower fill factor of this subcell, its current output must sufficiently exceed those of the upper two subcells (~17 mA/cm^2) in order to maximize the contribution from the bottom subcell. For the case of a 4J IMM cell, this requirement is considerably relaxed, since the current density of the upper 3 subcells is reduced by a factor of 2/3 compared to the 3J IMM case. Consequently, it is feasible to utilize a ~1.1 eV metamorphic subcell for the 4J IMM structure.

In a conventional 3J cell where Ge is the bottom subcell, its current output is approximately twice that of the top and middle subcells, and as such, the Ge subcell contributes optimally to the overall 3J device. The situation for the 3J IMM cell in this regard, is similar to that of a conventional 3J cell where an IRR (infrared reflecting) coating is applied such that a portion of the incident sunlight used by the Ge subcell is prevented from entering the cell [7]. In reference [7], the impact of the overall 3J device performance as a function of the IR cut-off wavelength (which effectively lowers the Ge current output) was studied. For the 3J IMM device, this effect should be carefully considered in order to choose the optimal bandgap for the $Ga_{1-x}In_xAs$ bottom subcell. For the 4J IMM device, the current density requirement from the 1 eV junction is substantially reduced and offers a design that is likely to produce higher fill factor devices. An important benefit that may be realized for IMM solar cells is the lower absorptance (confirmed by actual measurements), leading to lower operating cell temperatures and enhanced performance.

IMM solar cell performance

Figure 5 shows the measured light IV curve of a 4 cm^2 3J IMM solar cell device, with V_{oc} = 2.963 V, J_{sc} = 16.90 mA/cm^2, FF = 82.5%, and AM0 Eff = 30.5%. The device layers were grown by MOVPE on a standard Ge solar cell substrate (175 µm thick, 100 mm diameter), then mounted onto a handle substrate (another Ge in this case), then processed into 2 cm x 2 cm cells. Several other cells within the same wafer showed electrical performance approaching the best cell shown in the figure, demonstrating good uniformity across a reasonably large area, and highlighting the advances in the MOVPE growth as well as cell processing techniques for the IMM technology at Spectrolab.

The measured EQE curves from the top, middle, and bottom subcells of the 30.5%-efficiency cell are shown in Figure 6, indicating that the current densities of the top, middle, and bottom subcells are 17.0, 16.8, and 17.0 mA/cm^2, respectively). It is noted that the current density of the current limiting cell (16.8 mA/cm^2) is within 1% of the J_{sc} of the light IV measurement.

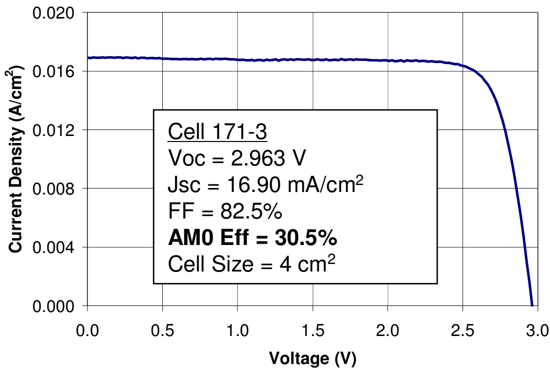

Figure 5. Measured light IV curve of a 4 cm^2 3J IMM solar cell device, with AM0 efficiency of 30.5%.

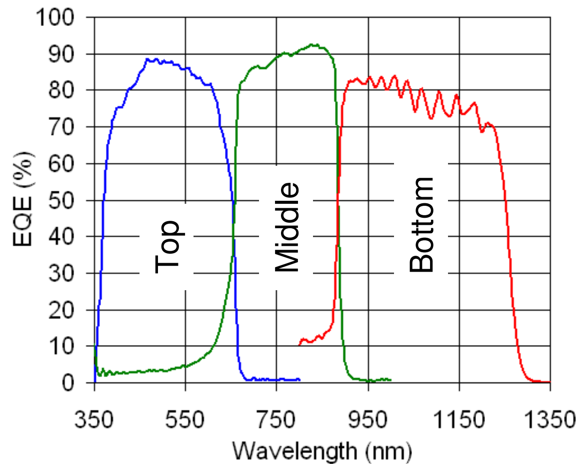

Figure 6. Measured EQE curves from the top, middle, and bottom subcells of the 30.5%-efficiency device shown in Figure 5. The current densities for the GaInP top, GaInAs middle, and GaInAs bottom subcells are 17.0, 16.8, and 17.0 mA/cm^2, respectively.

In addition to the above 3J IMM solar cell results, we have demonstrated 4J IMM 1 cm x 1 cm devices with V_{oc} reaching 4.0 V, with excellent uniformity across the entire 100 mm diameter wafer. While these initial results are very promising, they have also identified clear improvement areas that will help realize the full performance potential from the IMM solar cells. For example, the current density of the top and middle subcells of the 3J IMM device is expected to reach >17 mA/cm^2 upon optimization of these subcells. Higher voltage from the top subcell for both 3J and 4J IMM can be realized by using AlGaInP. Further optimization of the bottom subcell including the buffer layer, is expected to increase the voltage and the current output from this subcell. All of these improvements coupled with optimization of MOVPE growth conditions are expected to enable the IMM technology to demonstrate 33% AM0 efficiency in the near future.

Summary

The progress in the development of IMM solar cells at Spectrolab has been summarized. We have demonstrated 30.5% AM0 efficiency based on the 3J IMM cell architecture grown on a Ge substrate, with V_{oc} = 2.963 V, J_{sc} = 16.90 mA/cm^2, and FF = 82.5%. 4J IMM solar cells with V_{oc} reaching 4.0 V have also been demonstrated. Uniform device performance has been demonstrated across large wafer areas in a repeatable manner. These encouraging results indicate that the IMM cell architecture could serve as the platform for the next generation, high-efficiency solar cells.

Acknowledgments

The authors would like to thank Henry Yoo and John Merrill of the Air Force Research Laboratory (AFRL/VS), Jennifer Granata of the Aerospace Corporation, and Chris Fetzer, Takahiro Isshiki, Irma Valles, Mark Takahashi, and the entire multijunction solar cell team at Spectrolab. This work was supported in part by AFRL/VS under, contract #FA9453-06-C-0344, contract #FA9453-04-2-0042, and by Spectrolab.

References

[1] C. Fetzer, B. Jun, K. Edmondson, S. Khemthong, K. Rouhani, R. Cravens, R. Bardfield, and M. Gillanders, "Production 30% efficient triple junction space solar cells", this conference.

[2] R. R. King, C. M. Fetzer, D. C. Law, K. M. Edmondson, H. Yoon, G. S. Kinsey, D. D. Krut, J. H. Ermer, P. Hebert, B. T. Cavicchi, and N. H. Karam, "Advanced III-V Multijunction Cells for Space", *Proc. 4th World Conf. on Photovoltaic Energy Conversion*, Waikoloa, Hawaii, May 7-12, 2006, p. 1757-62.

[3] R.R. King, D.C. Law, K.M. Edmondson, C.M. Fetzer, G.S. Kinsey, H. Yoon, R.A. Sherif, and N.H. Karam, "40% efficient metamorphic GaInP/GaInAs/Ge multijunction solar cells, *Appl. Phys. Lett.* **90**, 183516 (2007).

[4] H. Yoon, C. M. Fetzer, D.C. Law, K.M. Edmondson, R. R. King, D. Krut, S. Mesropian, D. Bhusari, M. Haddad, T. Isshiki, J. Yen, X. Zhang, J. Hoskin, M. Lau, G. Kinsey, P. Hebert, and N.H. Karam, "Multijunction Space Solar Cells with 30% Efficiency and Beyond," presented at the *Space Power Workshop*, Apr. 23-26, 2007, Los Angeles, CA, USA.

[5] J.F. Geisz, Sarah Kurtz, M.W. Wanlass, J.S. Ward, A. Duda, D.J. Friedman, J.M. Olson, W.E. McMahon, T.E. Moriarity, and J.T. Kiehl, "High-efficiency GaInP/ GaAs/InGaAs triple-junction solar cells grown inverted with a metamorphic bottom junction, *Appl. Phys. Lett.* **91**, 023502 (2007).

[6] P. Sharps, "Surpassing the 30% Efficiency Level for Multi-Junction Space Solar Cells," presented at the *Space Power Workshop*, Apr. 23-26, 2007, Los Angeles, CA, USA.

[7] H. Yoon, D.E. Joslin, D.C. Law, D. Krut, R.R. King, P. Vijayakumar, D. Peterson, J. Hanley, and N.H. Karam, "Application of infrared reflecting (IRR) coverglass on multijunction III-V solar cells," *Proc. 4th World Conf. on Photovoltaic Energy Conversion*, Waikoloa, Hawaii, May 7-12, 2006, pp.1861-1864.